CEE'07 - 2nd INTERNATIONAL CONFERENCE ON ELECTRICAL ENGINEERING
ISBN: 978-972-99064-4-2

HELICOPTER SYSTEM MODELLING AND CONTROL WITH MATLAB

J. Coelho, R. Neto, D. Afonso, C. Lebres, H. Fachada, N. M. Fonseca Ferreira(1)

E. J. Solteiro Pires(2), J. A. Tenreiro Machado(3)

Institute of Engineering of Coimbra, PORTUGAL[1]
University of Trás–os–Montes and Alto Douro, PORTUGAL[2]
Institute of Engineering of Porto, PORTUGAL[3]

Abstract: This paper presents the modelling and control of a laboratory helicopter system with MatLab. In this perspective, students are motivated to investigate the dynamics, trajectory planning and control. Based on this experience, further studies on helicopter system, using more sophisticated concepts, are, then, more attractive from the students point of view.

Keywords: **Helicopter, model, PID, Fuzzy control**

1. Introduction

Da Vinci is credited with the design of the first helicopter, basically a helical air screw (figure 1), which was conceived to lift off the ground vertically. However, nearly four centuries later, when technology advancements allowed sustained, powered manned flight, the practical solution demonstrated by the Wright brothers used a fixed-surface to provide the lift. This required the aircraft to accelerate along the ground until a sufficient speed was reached, so that the necessary force could be generated for the vehicle to become airborne.

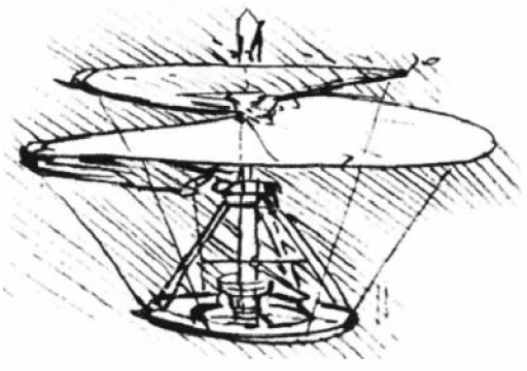

Figure 1 – The first helicopter helical air screw.

Historical flight documents have hundreds of failed helicopter projects [1]. Most of them were made based on hope in flying at any cost. However, some of these designs provided a significant contribution to a new understanding that ultimately led to the successful improvement of the modern helicopter. Yet, it was not until the more technical contributions of engineers such as Juan de la Cierva, Henrich Focke, Raoul Hafner, Harold Pitcairn, Igor Sikorsky, Arthur Young, and others, that the design of a truly safe and practical helicopter becomes a reality [2].
Sikorsky described seven fundamental technical problems that limited early experiments with helicopters.
Understanding the basic aerodynamics of vertical flight. The theoretical power required to produce a fixed amount of lift was an unknown quantity to the earliest experimenters, who were guided more by intuition than by science.
Another problem was the lack of a suitable engine, which was solved through the development of practical internal combustion (gasoline-powered) engines in the twentieth century. The structural weight and the engine weight down so the machine could lift a pilot and a payload. Early power motors were made of cast iron and were heavy. Aluminium was not available commercially until about 1890.
The counteracting rotor – torque reaction was another problem. The relatively simple idea of a tail rotor, to counter torque reaction, was not used on most early helicopter designs; these machines were either coaxial or side-by-side rotor configurations. Yet, building and controlling two or more primary lifting rotors was even more difficult than controlling one rotor, a fact that seemed to evade many inventors and constructors. Providing stability and properly controlling the machine, including a means of defeating the unequal lift produced on the blades advancing into and retreating from the relative wind when in forward flight. These were problems that were only to be fully overcome with the use of blade articulation, ideas that were pioneered by Cierva, Breguet, and others, and with the development of practical forms of cyclic blade pitch control by Hafner and others. The vibrations were a source of many mechanical failures of the rotor and airframe because of an insufficient understanding of the dynamic and aerodynamic behaviour of rotating wings. Other problem is the safety capability in the event of engine failure. It is fair to say that this capability is critical to the success of any practical helicopter, or other type of rotorcraft, because it would simply not be accepted otherwise.

ISBN: 978-972-99064-4-2

The relatively high weight of the structure, engine, and transmission was mainly responsible for the painfully slow initial development of the helicopter. In particular, the success of the helicopter had to wait until aircraft engine technology could be refined to the point that lightweight engines, with considerable power, could be built. By 1920, gasoline-powered reciprocating engines, with higher power-to-weight ratios were more widely available and the anti-torque and control problems of achieving successful vertical flight were at the forefront.
This resulted in the development of a vast number of prototype helicopters. Many of the early designs were built in Britain, France, Germany, and Italy, that led the field in several technical areas. One of the most important advances of all was in engine technology, with powerful reciprocating and gas turbine (turboshaft) engines, the latter of which revolutionized both fixed-wing and rotating-wing borne flight.

Recent years have witnessed a rapid progress in the enabling technologies for unmanned aerial vehicles. Those include airframes, propulsion systems, payloads, safety or protection systems, launch and recovery, data processor, ground control station, navigation and guidance, and autonomous flight controllers. From all those factors, system technology occupies the most critical contribution to the success of unmanned aerial vehicles (UAV) development and operation.

Creating reliable helicopter systems control is not an easy task, because, in general, we are talking about MIMO systems. In figure 7, we can see a MIMO Block Diagram of the Twin Rotor helicopter system control. The helicopter model consists of a common core of rigid-body dynamics equations, main and tail rotors flapping dynamics and aerodynamics, a mathematical model that provides the aerodynamic forces and moments.
The helicopter model adopted in this paper is a highly nonlinear two inputs and two output system [3, 4]. This system can also lead to very complicated models and several methods could have been used to derive its dynamics.
This paper presents several control techniques for a lab helicopter model, illustrated in Figure 2 and 3. For that propose we consider the helicopter, the Twin Rotor Mimo System (Feedback TRMS) and the conventional *PID* and *Fuzzy Logic* controllers.

Figure 2 – Two views of the twin rotor MIMO System.

The paper is organized as follows. Section two, provides an overview of the system model. Section three shows the classical and the fuzzy controllers. Section four presents simulated results. Finally, section five outlines the conclusions.

2. Helicopter model

We consider the rotation of the beam in a vertical plane, i.e., around the horizontal axis. Having in mind that the driving torques produced by the propellers, the rotation can be described in principle like the motion of a pendulum.

Table I – Helicopter Model Nomenclature

Variable	Description	Units[SI]
α_h	Horizontal position (azimuth position) of the model beam	[rad]
Ω_h	Angular velocity (azimuth velocity) of the model beam	[rad/s]
U_h	Horizontal DC-motor voltage control input	[V]
G_h	Linear transfer function of tail rotor DC-motor	
H	Non-linear part of DC- motor with tail rotor	[rad/s]
ω_h	Rotational speed of tail rotor	[rad/s]
F_h	Non-linear function (quadratic) of aerodynamic force from tail rotor	[N]
l_h	Effective arm of aerodynamic force from tail rotor	[m]
J_h	Non-linear function of moment of inertia with respect to vertical axis	[Kg.m^2]
M_h	Horizontal turning torque	[N.m]
K_h	Horizontal angular momentum	[N.m.s]
f_h	Moment of friction force in vertical axis	[N.m]
α_v	Vertical position (Pitch position) of the model beam	[rad]
Ω_v	Angular velocity (Pitch velocity) of the model beam.	[rad/s]
U_v	Vertical DC-motor voltage control input	[V]
G_v	Linear transfer function of main rotor DC-motor	
v	Non-linear part of DC-motor with main rotor	[rad/s]
ω_v	Rotational speed of main rotor	[rad/s]
F_v	Non-linear function (quadratic) of aerodynamic force from main rotor	[N]
l_v	Arm of aerodynamic force from main rotor	[m]
J_v	Moment of inertia with respect to horizontal axis	[Kg.m^2]
M_v	Vertical turning moment	[N.m]
K_v	Vertical angular momentum	[N.m.s]
f_v	Moment of friction force in horizontal axis	[N.m]
f	Vertical turning moment from counterbalance	[N.m]
J_{hv}	Vertical angular momentum from tail rotor	[N.m.s]
J_{vh}	Horizontal angular momentum from tail rotor	[N.m.s]
g_{vh}	Non-linear function (quadratic) of reaction turning	[N.m]
g_{hv}	Non-linear function (quadratic) of reaction turning	[N.m]
t	Time	[s]
$1/s$	Transfer function of an integrator	

ISBN: 978-972-99064-4-2

The physical model is developed under some simplifying assumptions. Furthermore, it is assumed that friction in the system is of the viscous type. It is assumed also that the propeller air subsystem could be described in accordance with the postulates of flow theory.

First, consider the rotation of the beam in the vertical plane, around the horizontal axis. Having in mind that the driving torques is produced by the propellers, the rotation can be described in principle as the motion of a pendulum.
From Newton´s second law of motion we obtain:

$$M_v = J_v \frac{d^2\alpha_v}{dt^2} \tag{1}$$

where M_v is the total moment of forces in the vertical plane, J_v is the sum of moments of inertia to the horizontal axis α_v is the pitch angle of the beam and:

$$M_v = \sum_{i=1}^{4} M_{vi} \tag{2a}$$

$$J_v = \sum_{i=1}^{8} J_{vi} \tag{2b}$$

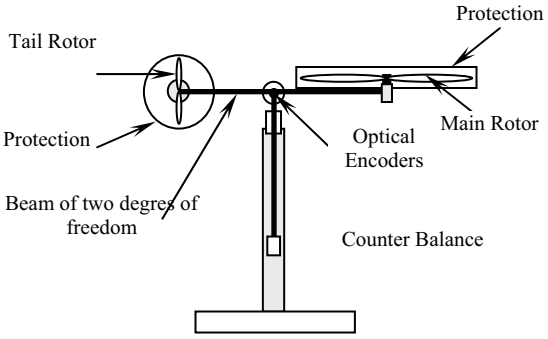

Figure 3 – The twin rotor mimo system.

To determine the moments of gravity forces applied to the beam, making it rotate around the horizontal axis, we consider the situation in figure 4, and:

$$M_{v1} = g[A - B]\cos\alpha_v - C\sin\alpha_v \tag{3a}$$

$$A = \left(\frac{m_t}{2} + m_{tr} + m_{ts}\right) l_t \tag{3b}$$

$$B = \left(\frac{m_m}{2} + m_{mr} + m_{ms}\right) l_m \tag{3c}$$

$$C = \frac{m_b}{2} l_b + m_{cb} l_{cb} \tag{3d}$$

where M_{v1} is the return torque corresponding to the forces of gravity, m_{mr} is the mass of the main DC-motor with main rotor, m_m is the mass of main part of the beam, m_{tr} is the mass of the tail motor with tail rotor, m_t is the mass of the tail part of the beam, m_{cb} is the mass of the counter-weight, m_b is the mass, of the counter-weight beam, m_{ms} is the mass of the main shield, m_{ts} is the mass of the tail shield, l_m is the length of main part of the beam, l_t is the length of tail part of the beam, l_b is the length of the counter-weight beam, l_{cb} is the distance between the counter-weight and the joint and g is the gravitational acceleration. Also:

$$M_{v2} = l_m F_v(\omega_m) \tag{4}$$

where M_{v2} is the moment of the propulsive force produced by the main rotor, ω_m is angular velocity of the main rotor and $F_v(\omega_m)$ denotes the dependence of the propulsive force on the angular velocity of the rotor.

$$M_{v3} = -\Omega_h^2 (A + B + C)\sin\alpha_v \cos\alpha_v \tag{5}$$

where M_{v3} is the moment of centrifugal forces corresponding to the motion of the beam around the vertical axis, and:

$$\Omega_h = \frac{d\alpha_h}{dt} \tag{6}$$

where Ω_h is the angular velocity of the beam around the vertical axis and is the azimuth angle of the beam. To determine the moments of propulsive forces applied to the beam consider the situation given in figure 5.

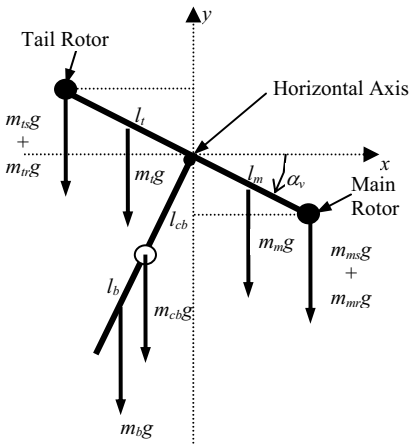

Figure 4 – Gravity forces in the TRMS, corresponding to the return torque, which determines the equilibrium position of the system.

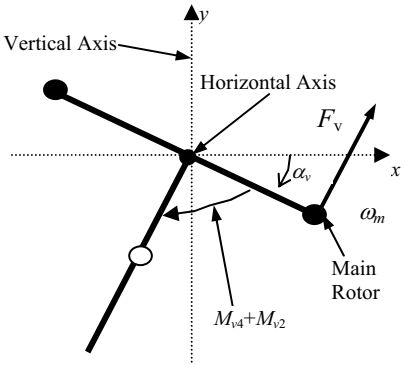

Figure 5 – Propulsive force moment and friction moment in the TRMS.

ISBN: 978-972-99064-4-2

Finaly:

$$M_{v4} = -\Omega_v K_v \tag{7}$$

where M_{v4} is the moment of friction depending on the angular velocity of the beam around the horizontal axis, and:

$$\Omega_v = \frac{d\alpha_{vh}}{dt} \tag{8}$$

where Ω_v is the angular velocity around the horizontal axis and K_v is a constant.
According to figure 5 we can determine components of the moment of inertia relative to the horizontal axis. Notice, that this moment is independent of the position of the beam.

$$J_{v1} = m_{mr} l_m^2 \tag{9a}$$

$$J_{v2} = m_m \frac{l_m^2}{3} \tag{9b}$$

$$J_{v3} = m_{cb} l_{cb}^2 \tag{9c}$$

$$J_{v4} = m_b \frac{l_b^2}{3} \tag{9d}$$

$$J_{v5} = m_{tr} l_t^2 \tag{9e}$$

$$J_{v6} = m_t \frac{l_t^2}{3} \tag{9f}$$

$$J_{v7} = \frac{m_{ms}}{2} r_{ms}^2 + m_{ms} l_m^2 \tag{9g}$$

$$J_{v8} = m_{ts} r_{ts}^2 + m_{ts} l_t^2 \tag{9h}$$

where r_{ms} is the radius of the main shield and r_{ts} is the radius of the tail shield.
Similarly, we can describe the motion of the beam around the vertical axis, having in mind that the driving torques are produced by the rotors and that the moment of inertia depends on the pitch angle of the beam. The horizontal motion of the beam (around the vertical axis) can be described as a rotational motion of a solid mass:

$$M_h = J_h \frac{d^2\alpha_h}{dt^2} \tag{10}$$

where, M_h is the sum of moments of forces acting in the horizontal plane, and J_h is the sum of moments of inertia relative to the vertical axis. Then:

$$M_h = \sum_{i=1}^{2} M_{hi} \tag{11}$$

$$J_h = \sum_{i=1}^{8} J_{hi} \tag{12}$$

To determine the moments of forces applied to the beam and making it rotate around the vertical axis, consider the situation shown in Figure 6.

$$M_{h1} = l_t . F_h(w_t) \cos\alpha_v \tag{13}$$

where ω_t is the rotational velocity of tail rotor, $F_h(\omega_t)$ denotes the dependence of propulsive force on the angular velocity of the tail rotor which should be determined experimentally, and:

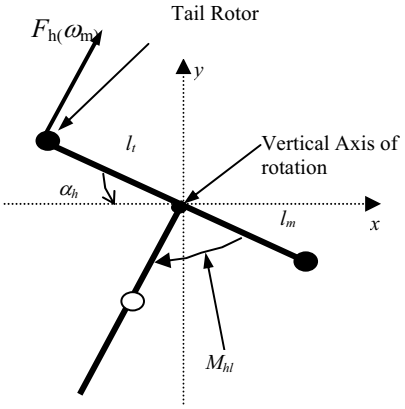

Figure 6 - Moments of forces in horizontal plane.

$$M_{h2} = -\Omega_h K_h \tag{14}$$

$$J_h = D\cos^2\alpha_v + E\sin^2\alpha_v + F \tag{16}$$

$$D = \frac{m_b}{3} l_b^2 + m_{cb} l_{cb}^2 \tag{17}$$

$$E = \left(\frac{m_m}{3} + m_{mr} + m_{ms}\right) l_m^2 + \left(\frac{m_t}{3} + m_{tr} + m_{ts}\right) l_t^2 \tag{18}$$

$$F = m_{ms} r_{ms}^2 + \frac{m_{ts}}{2} r_{ts}^2 \tag{19}$$

The helicopter motion can be describe by the equations:

$$\frac{dS_v}{dt} = \frac{l_m F_v(\omega_m) - \Omega_v K_v + G - H}{J_v} \tag{20}$$

$$G = g\left[(A-B)\cos\alpha - C\sin\alpha_v\right] \tag{21}$$

$$H = \frac{1}{2}\Omega_h^2 (A+B+C)\sin 2\alpha_v \tag{22}$$

$$\frac{d\alpha_v}{dt} = \Omega_v \tag{23}$$

$$\Omega_v = \frac{S_v + J_{tr}\omega_t}{J_v} \tag{24}$$

$$\frac{dS_h}{dt} = \frac{l_t F_h(\omega_t)\cos\alpha_v - \Omega_h K_h}{J_h} \tag{25}$$

$$\Omega_h = \frac{d\alpha_h}{dt} \tag{26}$$

$$\Omega_h = S_h + \frac{J_{tmr}\omega_m \cos\alpha_v}{J_h} \tag{27}$$

ISBN: 978-972-99064-4-2

where J_{tr} is the moment of inertia in DC motor tail, J_{mr} is the moment of inertia in DV motor main, S_v is the angular momentum in vertical plane of the beam and S_h is the angular momentum in horizontal plane of the beam.
The angular velocities are a function of the DC motors, yielding:

$$\frac{du_{vv}}{dt} = \frac{1}{T_{mr}}\left(-u_{vv} + u_v\right) \tag{28}$$

$$\omega_m = P_v(u_{vv}) \tag{29}$$

$$\frac{du_{hh}}{dt} = \frac{1}{T_{tr}}\left(-u_{hh} + u_h\right) \tag{30}$$

$$\omega_t = P_h(u_{hh}) \tag{31}$$

where T_{mr} is the time constant of the main motor and T_{tr} is the time constant of the tail motor.
Finally, the mathematical model becomes a set of six non-linear equations, namely:

$$\mathbf{U} = \left[U_h \; U_v\right]^T \tag{32}$$

$$\mathbf{X} = \left[S_h \; \alpha_h \; u_{hh} \; S_v \; \alpha_v \; u_{vv}\right]^T \tag{33}$$

$$\mathbf{Y} = \left[\Omega_h \; \alpha_h \; \omega_t \; \Omega_v \; \alpha_v \; \omega_m\right]^T \tag{34}$$

where **U** is the input, **X** is the state and **Y** is the output vector.

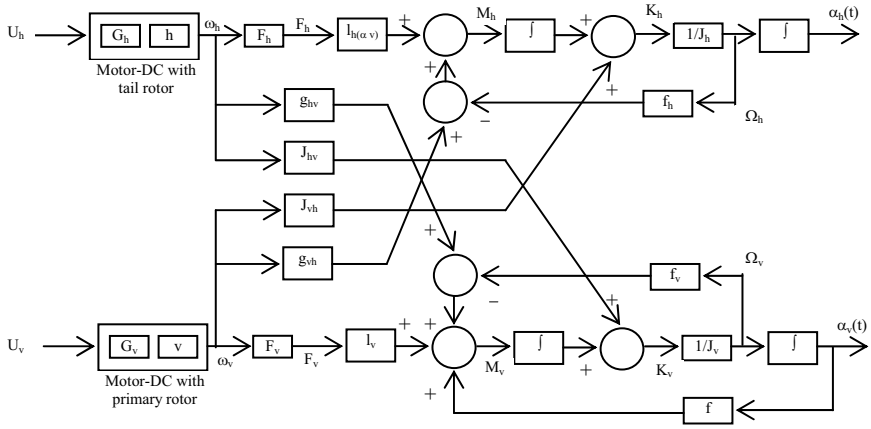

Figure 7 – The MIMO Block Diagram of the Twin Rotor

3. Twin Rotor MIMO Controllers

3.1. PID controllers

The *PID* controllers are the most commonly used control algorithms in industry. Among the various existent schemes for tuning *PID* controllers, the Ziegler-Nichols (Z-N) method is the most popular and is still extensively used for the determination of the PID parameters. It is well known that the compensated systems, with controllers tuned by this method, have generally a step response with a high percent overshoot. Moreover, the Z-N heuristics are only suitable for plants with monotonic step response [5-7].
The transfer function of the PID controller is:

$$G_c(s) = \frac{U(s)}{E(s)} = K\left(1 + \frac{1}{T_i s} + T_d s\right) \tag{35}$$

where $E(s)$ is the error signal and $U(s)$ is the controller's output. The parameters K, T_i, and T_d are the proportional gain, the integral time constant and the derivative time constant of the controller, respectively.
The design of the *PID* controller will consist on the determination of the optimum *PID* set gains (K, T_i, T_d) that minimize J, the integral of the square error (ISE), defined as:

$$J = \int_0^\infty \left\{\left[\alpha_h(t) - \alpha_{hd}(t)\right]^2 + \left[\alpha_v(t) - \alpha_{vd}(t)\right]^2\right\} dt \tag{36}$$

where $\alpha_i(t)$ is the step response of the closed-loop system with the *PID* controller and $\alpha_{id}(t)$ is the desired step response.

The control architecture can be resumed in the block diagram of figure 8, with the two independent controllers.

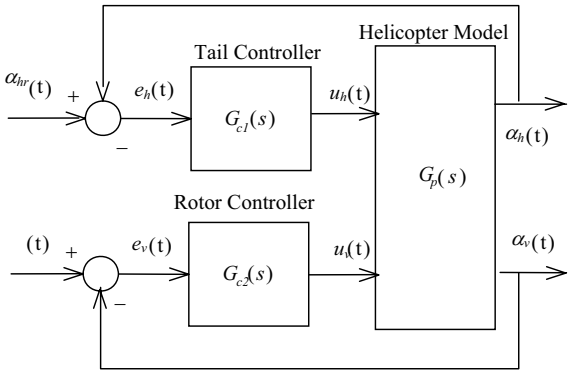

Figure 8 –Twin Rotor Mimo Block *PID* Control Diagram.

ISBN: 978-972-99064-4-2

3.2. Fuzzy Controllers

Basically, Fuzzy Logic (*FL*) is a multivalued logic that allows intermediate values to be defined between conventional evaluations like 'true' or 'false', 'yes' or 'no', 'high' or 'low'. Notions like 'rather tall' or 'very fast' can be formulated mathematically and processed by computers, in order to apply a more humanlike way of thinking in the programming of computers. The introduction of fuzzy concepts was set by Lotfi Zadeh (1965), since then *FL* controllers have received considerable interest from many researchers [8-13].

FL has emerged as a profitable tool for the controlling and steering of systems and complex industrial processes, as well as for household and entertainment electronics and expert systems and applications such as the helicopter control.

For each *FL* controller of the helicopter we have two inputs, one output and six fuzzy rules (Table II). Each of the inputs has a membership function (as shown in Figure 9). The input from the encoders is passed on this membership functions to generate input fuzzy variables, which are then normalize to evaluate the fuzzy rules and to generate the output fuzzy variables. Output fuzzy variables are then defuzzied to generate output for both main and tail rotors.

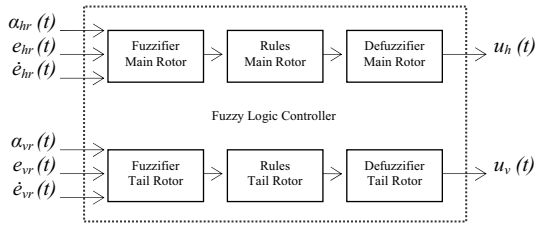

Figure 9 – Twin Rotor Mimo *FL* Block Control Diagram

For both fuzzy controllers we have 2 inputs, which are the position error and the error variation.

Table II – Fuzzy Logic Main Rotor Control Rule.

		Position Error		
		P	**Z**	**N**
Error Variation	**P**	V_OP	V_OZ	V_OP
	Z	V_OP	V_OZ	V_ON
	N	V_ON	V_OZ	V_ON

The labels stand for **P** Positive, **Z** Zero, **N** Negative and $\mathbf{V_OP/Z/N}$ Voltage Output Positive, Zero and Negative. The membership functions chosen are Gaussian with equidistant centres over the interval [–1, +1].

4. Controller Performances

In this section we analyze the system performance; furthermore, we compare the response of classical *PID* and *FL* controllers. For the *PID* case we adopt the parameters of table III.

Table III –The *PID* control gains.

Parameters	**Main**	**Tail**
$\mathbf{K_P}$	14.5	10.0
$\mathbf{K_I}$	10.7	3.7
$\mathbf{K_D}$	7.0	8.0

In order to study the system dynamics, we apply, separately, a step perturbation, at the tail and main rotor references, that is, we perturb the reference with $\{\delta\alpha_h,\delta\alpha_v\} = \{12^o,0\}$ and $\{\delta\alpha_h,\delta\alpha_v\} = \{0^o,12^o\}$. In all experiments we consider the same controller sampling frequency $f_c = 1$ kHz, and the operating point of the object $\alpha_h = 24$ degrees and $\alpha_v = 24$ degrees. Figures 10 and 11 show the time response for a step perturbation.

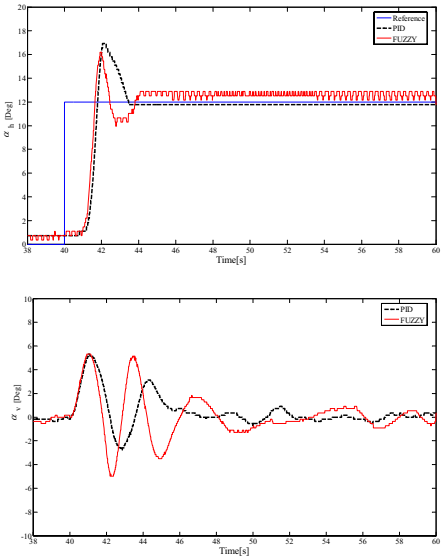

Figure 10 – Time response of α_v and α_h using the *PID* and *FL* controllers, for a pulse perturbation at the α_{hr} position reference $\delta\alpha_h = 12^o$.

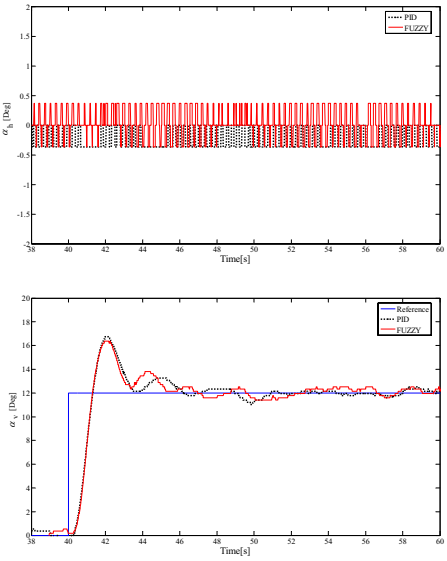

Figure 11 – Time response of α_v and α_h using the *PID* and *FL* controllers, for a perturbation at the α_{vr} position reference, $\delta\alpha_v = 12^o$.

ISBN: 978-972-99064-4-2

Figure 12 shows the quadratic error ($\varepsilon_{h,v}$) for trajectory perturbation, at the tail and main rotor references.

$$\varepsilon_h = \sqrt{\left(\delta\alpha_{h\,ref} - \alpha_h\right)^2 + \left(\alpha_{v\,ref} - \alpha_v\right)^2} \qquad (37)$$

$$\varepsilon_v = \sqrt{\left(\alpha_{h\,ref} - \alpha_h\right)^2 + \left(\delta\alpha_{v\,ref} - \alpha_v\right)^2} \qquad (38)$$

where $\varepsilon \equiv \{\varepsilon\delta_h, \varepsilon\delta_v\}$ represent the corresponding perturbations in the variables $\{\delta\alpha_h, \delta\alpha_v\}$, respectively.

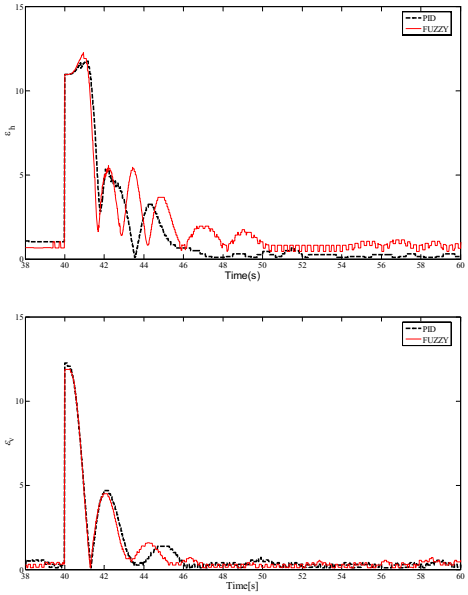

Figure 12 – Quadratic error ($\varepsilon_{h,v}$) for trajectory perturbation, at α_h and α_v rotor references, using the *PID* and *FL* controllers.

The time responses characteristics, namely the percent overshoot *PO%*, the steady-state error e_{ss}, the peak time T_p, the rise time T_r and the settling time T_s, are presented in (Tables IV and V).

Table IV – Main rotor response parameters

	PO(%)	e_{SS} (º)	t_r (s)	t_p (s)	t_s (s)
PID	41.6	0.2	0.6	2.1	2.4
FUZZY	34.2	0.9	0.5	1.9	3.0

Table V – Tail rotor response parameters

	PO(%)	e_{SS} (º)	T_r (s)	T_p (s)	t_s (s)
PID	40.0	0.5	1.2	2.2	12.0
FUZZY	36.6	1.2	1.2	2.2	12.0

Figures 13 and 14 show the voltage statistical distribution at main rotor and tail for both controllers. The standard deviation can be obtained by:

$$\sigma = \sqrt{\frac{\left(U_i - \mu\right)^2}{N}} \qquad (39)$$

where U_i is voltage input, N is the number of samples, μ represent the sample mean and σ is the standard deviation.

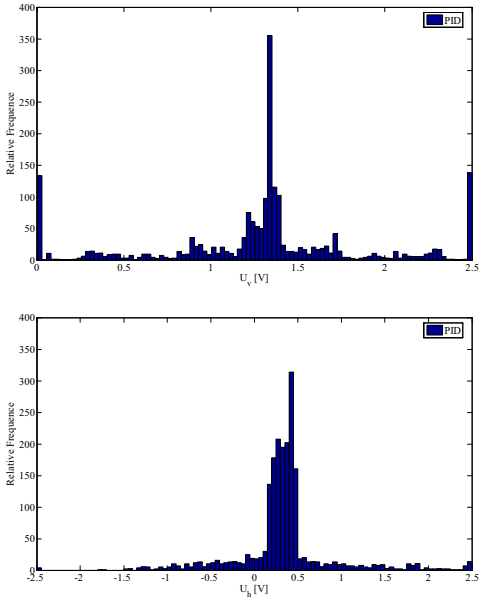

Figure 13 – Rotor and tail voltage statistical distribution of the control action using the *PID* controller.

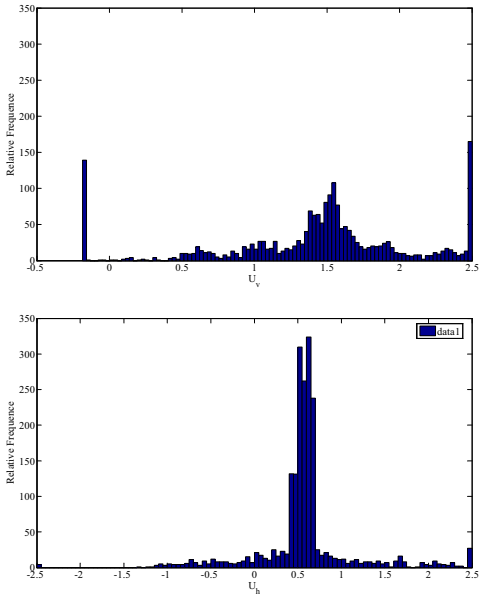

Figure 14 – Rotor and tail voltage statistical distribution of the control action using the *FL* controller.

The control system using the *FL* controller presents higher voltage, for main rotor perturbation, μ_{FL} = 1.75V and σ_{FL} = 0.66, comparing with the *PID* controller μ_{PID} = 1.32V and σ_{FL} = 0.59. But for tail rotor perturbation the *FL* controller presents better results μ_{FL} = 0.15V, σ_{FL} = 0.41 and μ_{PID} = 0.35V, σ_{FL} = 0.44.

ISBN: 978-972-99064-4-2

Figure 15 shows the time response for a sinusoidal trajectory in references, α_v and α_h.

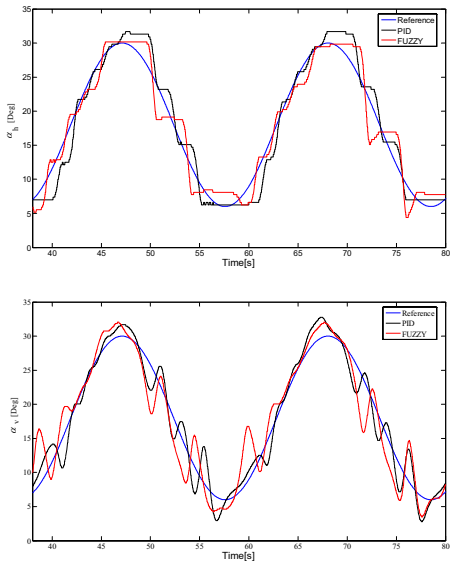

Figure 15 – Time responses of α_v and α_h using the *PID* and *FL* controllers, for a sinusoidal reference at α_v and α_h.

5. Conclusions

The conventional *PID* controller has better performance than the *FL* controller, but depends on the control table.
The performance was evaluated by introducing a small perturbation and the results demonstrated good performance for the *PID* and the *FL* controller. However, both controllers reveal same overshoot in the output responses and the *FL* needs more energy to perform the same task.

References

[1] J. Gordon Leishman, *Principles of Helicopter Aerodynamics*, Second Edition, Cambridge University Press.

[2] Martin D. Maisel, Demo J. Giulianetti and Daniel C. Dugan, *The History of the XV-15 Tilt Rotor Research Aircraft From Concept to Flight*, National Aeronautics and Space Administration Office of Policy and Plans NASA History Division Washington, D.C.2000.

[3] Feedback Instruments Ltd. Manual: 33-007-1C Ed04, 2002.

[4] M. López Martínez, F.R. Rubio (2004), *Approximate Feedback Linearization of a Laboratory Helicopter*, Sixth Portuguese Conference on Automatic Control, pp.43-45, Faro, Portugal

[5] Åström, K., Hang, C., Persson, P. and Ho,W. (1992). *Towards intelligent PID control*, Automática 28(1): 1–9.

[6] Åström, K. J. and Hägglund, T. (1995). *PID controller-Theory, Design and Tuning*, second edn, Instrument Society of America, 67 Alexander Drive, POBox 12277, Research Triangle Park, North Carolina 27709, USA.

[7] Åström, K. J. and Wittenmark, B. (1984). *Computer Controlled Systems, theory and Design*, Prentice-Hall, Englewood Cliffs.

[8] Islam, B.U.; Ahmed, N.; Bhatti, D.L.; Khan, S., *Controller design using fuzzy logic for a twin rotor MIMO system*, Multi Topic Conference, 2003. INMIC2003. 7th Internationa,lVolume , Issue , 8-9 Dec. 2003 Page(s): 264 – 268.

[9] Przemysław Gorczyca, Krystyn Hajduk, *Tracking Control Algorithms For A Laboratory Aerodynamical System*, Int. J. Appl. Math. Comput. Sci., 2004, Vol. 14, No. 4, 469–475.

[10] Rahideh, A, Shaheed, M H, Proceedings of the I MECH E Part I Journal of Systems & Control Engineering, Volume 221, Number 1, January 2007 , pp. 89-101(13)

[11] Amaral, T.G.; Crisostomo, M.M.; Pires, V.F., *Helicopter motion control using adaptive neuro-fuzzy inference controller*, IEEE IECON 02 Volume: 3 , 5-8 Nov. 2002 , Page(s): 2090 -2095 vol.3

[12] Siler, W. and Ying, H. (1989). *Fuzzy control theory: The linear case*, Fuzzy Sets and Systems 33: 275–290.

[13] Tso, S. K. and Fung, Y. H. (1997). *Methodological development of fuzzy-logic controllers from multivariable linear control*, IEEE Trans. Systems Man & Cybernetics 27(3): 566–572.

Author addresses

J. Coelho, R. Neto, D. Afonso, Students of Department of Electrical Engineering, Instituto Superior de Engenharia de Coimbra, R. Pedro Nunes, Quinta da Nora, 3030-199 Coimbra, Portugal, email: joaobcoelho@hotmail.pt, email: rodolfonneto.gmail.com

C. Lebres, Eq. Prof. Adj., Institute of Engineering of Coimbra, Dept. of Electrotechnical Engineering, Quinta da Nora, 3030-199 Coimbra, Portugal, email: clebres@isec.pt

H. Fachada, Prof. Adj., Institute of Engineering of Coimbra, Dept. of Electrotechnical Engineering, Quinta da Nora, 3030-199 Coimbra, Portugal, email: hfachada@isec.pt

N. M. Ferreira, Eq. Prof. Adj., Institute of Engineering of Coimbra, Dept. of Electrotechnical Engineering, Quinta da Nora, 3030-199 Coimbra, Portugal, email: nunomig@isec.pt

E. J. Solteiro Pires, Professor Auxiliar, Universidade Trás–os–Montes e Alto Douro Ap 1013, 5000–911 Vila Real, Portugal, email: epires@utad.pt

J. A. Tenreiro Machado, Coordinator Professor, Institute of Engineering of Porto, Dept. of Electrotechnical Engineering, Rua Dr. Antonio Bernardino de Almeida, 4200-072 Porto, Portugal, email: jtm@isep.ipp.pt